



Cite this: *Org. Biomol. Chem.*, 2017, **15**, 5797

The effect of L-DOPA hydroxyl groups on the formation of supramolecular hydrogels†

Nicola Zanna,* Debora Iaculli and Claudia Tomasini *

Fmoc-L-DOPA-D-Oxd-OH was prepared starting from commercially available L-DOPA. Its gelation ability was tested by comparison with Fmoc-L-Tyr-D-Oxd-OH and Fmoc-L-Phe-D-Oxd-OH using ten different triggers. Among them, only GdL, CaCl₂ and ZnCl₂ form strong hydrogels with the three gelators. The analysis of the aerogels obtained by freeze drying the hydrogels show that the three gelators always induce the formation of dense networks, which strongly depend on the nature of the gelator. Rheological analysis of these samples demonstrates that stronger gels were obtained using the L-Tyr containing gelator, while the L-DOPA containing hydrogels were characterized by a storage modulus approximately one order of magnitude lower. Finally, the L-Phe containing gelators show a different trend with respect to the other samples depending on the trigger used. All the hydrogels show a thixotropic behaviour at the molecular level. These results indicate that hydrogel formation is sensitive to both the number of the hydroxyl moieties on the aromatic rings and trigger used.

Received 28th April 2017,
Accepted 13th June 2017

DOI: 10.1039/c7ob01026e

rscl.li/obc

Introduction

In order to understand aggregation phenomena, oligopeptides may be designed and prepared either to mimick^{1–10} or interfere with^{11–13} these processes. The non-proteinogenic amino acid 3,4-dihydroxyphenyl-L-alanine (L-DOPA) contains the catechol moiety, which has a peculiar property to form stable complexes with metal cations.¹⁴ This property is responsible for the ability of marine mussels to attach to hard surfaces in the sea by means of byssus, which is a mixture of proteins rich in DOPA.¹⁵ The adhesion strength of byssus is also given by its ability to remove interfacial water from the target surfaces.¹⁶

Although various synthetic DOPA containing hydrogels have been reported, they comprise polymeric materials, whose gelation process is activated by high pressure,¹⁷ high temperature,¹⁸ large change in the pH value,¹⁹ and redox reagents.²⁰

(4*R*,5*S*)-4-Methyl-5-carboxy-oxazolidin-2-one moiety (D-Oxd) can be successfully utilized in the formation of several supramolecular materials,^{21–23} including hydrogels.^{24–26} This little molecule, which mimics a proline group, may form oligomers with stable secondary structures in solution due to its ability to fix the peptide bond in its *trans* conformation.^{27–29} Recently, we reported the gelation behavior of Fmoc-protected dipeptides, all containing the D-Oxd moiety, and we demon-

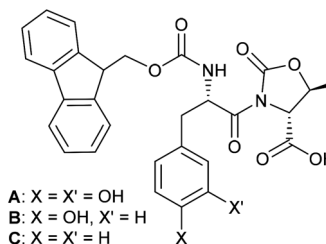


Fig. 1 The chemical structure of the three gelators A, B and C described in this study.

strated that good results may be obtained with dipeptides containing L-Phe or L-Tyr.^{30,31}

In this study, we describe the preparation of physical hydrogels^{32–35} using the L-DOPA containing pseudopeptide A (Fig. 1) as a gelator. We also compare its ability to form supramolecular hydrogels with the L-Phe and L-Tyr containing gelators B and C.

Experimental

Materials

All chemicals and solvents were purchased from Sigma-Aldrich, VWR or Iris Biotech and used as received. Acetonitrile was distilled under an inert atmosphere prior to use. MilliQ water (Millipore, resistivity = 18.2 mΩ cm) was used throughout. All solvents were dried by distillation before use. All reactions were carried out in dried glassware. The melting points

Dipartimento di Chimica "G. Ciamician" - Alma Mater Studiorum Università di Bologna, Via Selmi 2, 40126 Bologna, Italy. E-mail: claudia.tomasini@unibo.it
† Electronic supplementary information (ESI) available. See DOI: 10.1039/c7ob01026e

of the compounds are uncorrected. High quality infrared spectra (64 scans) were obtained using an ATR-FT-IR Bruker Alpha System spectrometer (64 scans). The spectra were obtained in 3 mM solutions in dichloromethane or as solids at 297 K. All compounds were dried *in vacuo*, and all the sample preparations were performed under a nitrogen atmosphere. NMR spectra were recorded on a Varian Inova 400 spectrometer at 400 MHz (^1H NMR) and 100 MHz (^{13}C NMR). Chemical shifts are reported in δ values relative to the solvent peak.

Boc-L-DOPA-OMe

The molecule was prepared and characterized according to a literature procedure.³⁶

Boc-L-DOPA(OBn)₂-OH

The molecule was prepared and characterized according to a literature procedure.³⁶

Boc-L-DOPA(OBn)₂-D-Oxd-OBn

To a stirred solution of Boc-L-DOPA(OBn)₂-OH (466 mg, 0.98 mmol) and HBTU (400 mg, 1.07 mmol) in dry acetonitrile (10 mL) under an inert atmosphere, H-D-Oxd-OBn (229 mg, 0.98 mmol) in dry acetonitrile (5 mL) was added at room temperature, together with DIPEA (349 μL , 2.05 mmol). The reaction was monitored *via* thin layer chromatography; when the reaction was complete, acetonitrile was removed under reduced pressure. Then, the crude mixture was dissolved in dichloromethane (30 mL) and washed with water (30 mL), 1 N aqueous HCl (30 mL) and 5% aqueous NaHCO₃ (30 mL), dried over anhydrous Na₂SO₄, filtered and concentrated *in vacuo*. The obtained solid was dissolved in methanol (10 mL), ultrasonicated for 15 min and then filtered over a Gooch flask. The solid was washed with methanol (1 \times 20 mL), dissolved in dichloromethane to recover it from the filter and concentrated *in vacuo* to afford Boc-L-DOPA(OBn)₂-D-Oxd-OBn (576 mg, 0.83 mmol) as a white solid (85% yield).

M.p. = 171.6–172.0 °C; IR (3 mM in CH₂Cl₂): ν 3439, 1791, 1754, 1711, 1508, 1496 cm⁻¹; ^1H NMR (400 MHz, CDCl₃): δ 1.36 (d, J = 6.4 Hz, 3H, CH₃ Oxd), 1.40 (s, 9H, *t*-Bu), 2.81–2.94 (m, 1H, CHH β -DOPA), 2.96–3.09 (m, 1H, CHH β -DOPA), 4.25 (d, J = 3.9 Hz, 1H, CHN Oxd), 4.43–4.56 (m, 1H, CHO Oxd), 5.11 (s, 2H, CH₂Ph), 5.14 (s, 2H, CH₂Ph), 5.21 (s, 2H, CH₂Ph), 5.78 (s, 1H, CH α -DOPA), 6.69 (d, J = 8.2 Hz, 1H, CH Ar DOPA), 6.75–6.96 (m, 2H, CH Ar DOPA), 7.14–7.58 (m, 15H, ArH). ^{13}C NMR (100 MHz, CDCl₃): δ 21.1, 28.4, 38.8, 53.9, 61.9, 68.1, 71.3, 71.4, 73.6, 79.9, 115.1, 116.4, 122.5, 127.3, 127.6, 127.8, 127.9, 128.4, 128.5, 128.8, 129.1, 134.7, 137.3, 137.4, 148.2, 149.0, 151.2, 154.7, 167.5, 172.7. Anal. calcd for C₅₀H₄₄N₂O₉: C, 73.52; H, 5.43; N, 3.43. Found: C, 73.48; H, 5.41; N, 3.39.

Fmoc-L-DOPA(OBn)₂-D-Oxd-OBn

Trifluoroacetic acid (1.14 mL, 14.40 mmol) was added under an nitrogen atmosphere to a solution of Boc-L-DOPA(OBn)₂-D-Oxd-OBn (558 mg, 0.80 mmol) in dry dichloromethane (5 mL). After 4 h, the reaction was complete, dichloromethane

was removed under reduced pressure, and H-L-DOPA(OBn)₂-D-Oxd-OBn-CF₃CO₂H was obtained in quantitative yield. The crude product was dissolved in dichloromethane (20 mL), and Fmoc *N*-hydroxysuccinimide ester (270 mg, 0.80 mmol) and DIPEA (516 μL , 3.04 mmol) were added to the mixture and stirred at room temperature for 24 h. Then, dichloromethane (30 mL) was added to the mixture, which was then washed with water (30 mL), 1 N aqueous HCl (30 mL) and 5% aqueous NaHCO₃ (30 mL), dried over anhydrous Na₂SO₄, filtered and concentrated *in vacuo*. The obtained solid was dissolved in methanol (10 mL), ultrasonicated for 15 min and then filtered over Gooch flask. The solid was washed with methanol (1 \times 20 mL), dissolved in dichloromethane to recover it from the filter and concentrated *in vacuo* to afford Fmoc-L-DOPA(OBn)₂-D-Oxd-OBn (630 mg, 0.77 mmol) as a white solid (96% yield). M.p. = 160.1–160.3 °C; IR (3 mM in CH₂Cl₂): ν 3428, 1792, 1754, 1712, 1511 cm⁻¹; ^1H NMR (400 MHz, CDCl₃): δ 1.38 (d, J = 6.4 Hz, 3H, CH₃ Oxd), 2.88–2.98 (m, 1H, CHH β -DOPA), 3.02–3.13 (m, 1H, CHH β -DOPA), 4.14–4.23 (m, 1H, O-CH-CH₂-Fmoc), 4.23–4.33 (m, 2H, O-CH-CH₂-Fmoc), 4.33–4.43 (m, 1H, CHN Oxd), 4.48–4.57 (m, 1H, CHO Oxd), 5.08 (s, 2H, CH₂Ph), 5.12 (s, 2H, CH₂Ph), 5.19 (s, 2H, CH₂Ph), 5.41 (d, J = 8.6 Hz, 1H, NH DOPA), 5.87 (dd, J = 14.4, 8.6 Hz, 1H, CH α -DOPA), 6.69 (dd, J = 8.1, 2.0 Hz, 1H, CH Ar DOPA), 6.83 (d, J = 8.1 Hz, 1H, CH Ar DOPA), 6.87 (d, J = 2.0 Hz, 1H, CH Ar DOPA), 7.18–7.50 (m, 19H, ArH), 7.55 (d, J = 6.3 Hz, 2H, ArH Fmoc), 7.75 (d, J = 6.3 Hz, 2H, ArH Fmoc); ^{13}C NMR (100 MHz, CDCl₃): δ 21.2, 38.6, 47.2, 54.3, 61.9, 67.2, 68.2, 71.4, 71.4, 73.8, 115.1, 116.4, 120.0, 122.5, 125.3, 127.2, 127.3, 127.3, 127.5, 127.6, 127.8, 127.8, 127.9, 128.4, 128.5, 128.6, 128.8, 128.8, 134.6, 137.3, 137.4, 141.4, 144.0, 148.4, 149.1, 151.3, 167.4, 172.4. Anal. calcd for C₄₀H₄₂N₂O₉: C, 69.15; H, 6.09; N, 4.03. Found: C, 69.18; H, 6.08; N, 4.07.

Fmoc-L-DOPA-D-Oxd-OH A

To a stirred solution of Fmoc-L-DOPA(OBn)₂-D-Oxd-OBn (100 mg, 0.12 mmol) in a mixture of TFA:methanol 5:95 (100 mL), Pd/C (10% w/w, 10 mg) was added, and a vacuum was created inside the flask using a vacuum line. The flask was then filled with hydrogen using a balloon (1 atm). The solution was stirred for 90 min under hydrogen atmosphere. The mixture was then filtered and concentrated *in vacuo*, and the solid was dissolved in dichloromethane, sonicated and filtered over a Gooch flask. The solid was dissolved in methanol to recover it from the filter and concentrated *in vacuo* to afford Fmoc-L-DOPA-D-Oxd-OH (56 mg, 0.104 mmol) as a white solid (85% yield).

M.p. = 135.4–136.4 °C; IR (ATR-IR): ν 3325, 1783, 1689, 1604, 1517 cm⁻¹; ^1H NMR (400 MHz, CD₃OD): δ 1.44 (d, J = 6.4 Hz, 3H, CH₃ Oxd), 2.75 (dd, J = 13.5, 5.3 Hz, 1H, CH₂ β -DOPA), 3.01 (dd, J = 13.5, 5.4 Hz, 1H, CH₂ β -DOPA), 4.10–4.22 (m, 2H, O-CH-CH₂-Fmoc), 4.23–4.33 (m, 1H, O-CH-CH₂-Fmoc), 4.37 (d, J = 3.7 Hz, 1H, CHN Oxd), 4.62–4.73 (m, 1H, CHO Oxd), 5.76 (dd, J = 9.0, 5.3 Hz, 1H, CH α -DOPA), 6.62 (d, J = 8.3 Hz, 1H, CH-Ar DOPA), 6.67 (d, J = 8.3 Hz, 1H, CH-Ar DOPA), 6.78 (s, 1H, CH-Ar DOPA), 7.22–7.33 (m, 2H, ArH Fmoc), 7.33–7.41 (m, 2H, Ar-H Fmoc), 7.59 (d, J = 7.6 Hz, 2H, Ar-H Fmoc), 7.77

(d, $J = 7.7$ Hz, 2H, Ar-H Fmoc); ^{13}C NMR (100 MHz, CD_3OD): δ 21.2, 30.7, 38.9, 39.2, 56.1, 63.3, 68.1, 75.9, 116.2, 117.5, 120.7, 120.8, 122.1, 125.0, 126.2, 126.3, 127.9, 128.1, 128.6, 129.2, 142.4, 145.1, 145.2, 145.3, 146.1, 153.6, 157.9, 171.5, 174.1. Anal. calcd for $\text{C}_{19}\text{H}_{24}\text{N}_2\text{O}_9$: C, 53.77; H, 5.70; N, 6.60. Found: C, 53.73; H, 5.75; N, 6.62.

Conditions for the gel formation with a pH trigger

20 mg of compound **A**, **B** or **C** was placed in a test tube (diameter: 8 mm), and MilliQ water (≈ 0.95 mL) and 1 M aqueous NaOH (1 equiv.) were added to obtain a final volume of 1 mL. Then, the mixture was stirred and sonicated in turn for about 30 min until sample dissolution. Furthermore, glucono- δ -lactone (GdL: 1.1 equiv.) was added in one portion to the mixture. After a rapid mixing to allow the GdL to completely dissolve, the sample was allowed to stand quiescently until gel formation occurred.

Conditions for gel formation with an inorganic trigger

20 mg of compound **A**, **B** or **C** was placed in a test tube (diameter: 8 mm), and MilliQ water (0.5 mL) and a 1 M aqueous NaOH (1 equiv.) were added to obtain a final volume of 1 mL. The mixture was stirred until sample dissolution. The cationic trigger (0.3 equiv.) was added to the solution under rapid stirring and then, the tube was allowed to stand quiescently until gel formation occurred.

Conditions for gel formation with an amino acid trigger

20 mg of compound **A**, **B** or **C** was placed in a test tube (diameter: 8 mm), and the selected amino acid (1 equiv.) was added. Then, 1 mL of MilliQ water was added to the test tube under stirring, and after 1 min, the magnetic stirrer was removed and the tube was allowed to stand quiescently until gel formation occurred.

Conditions for T_{gel} determination

T_{gel} was determined by heating test tubes (diameter: 8 mm) containing the gel and a glass ball (diameter: 5 mm, weight: 165 mg) placed on the top. When the gel was formed, the ball was suspended on top. The T_{gel} is the temperature at which the ball started to penetrate inside the gel. Some hydrogel samples melted, producing a clear solution, while in other cases the gelator shrank and water was ejected, as syneresis occurred.

Aerogels preparation

Aerogels were prepared using the following procedure: 0.5 mL of the hydrogel was prepared directly into an Eppendorf test tube at room temperature. After the hydrogel was formed (test tube inversion), the sample was dropped into liquid nitrogen for 10 min and then freeze-dried for 24 h *in vacuo* (0.02 mBar) at -50 °C using a BENCHTOP Freeze Dry System CHRIST Alpha 1–2 LD Plus.

SEM analysis

Scanning electron microscopy images was recorded using a Hitachi 6400 field emission gun scanning electron microscope.

Rheology

Rheology experiments were carried out on an Anton Paar Rheometer MCR 102 using a parallel plate configuration (25 mm diameter). Experiments were performed at a constant temperature of 25 °C controlled using the integrated Peltier system and Julabo AWC100 cooling system. To keep the sample hydrated, a solvent trap was used (H-PTD200). Amplitude and frequency sweep analysis was performed with fixed gap value of 1 mm on the gel samples prepared directly on the upper plate of the rheometer. The samples were prepared the day before the analysis and left overnight under a controlled temperature of 20 °C to complete the gelation process. Oscillatory amplitude sweep experiments (γ : 0.01–100%) were carried out in order to determine the linear viscoelastic (LVE) range at a fixed frequency of 1 rad s^{-1} . Once the LVE of each hydrogel was established, frequency sweep tests were performed (ω : 0.1–100 rad s^{-1}) at a constant strain within the LVE region of each sample. To verify the thixotropic properties of the hydrogels, strain values within and over the crossover point region were consecutively applied to the hydrogels. The values of the applied strain were selected on the basis of the crossover point value obtained from amplitude sweep experiment of hydrogels 1–9.

Results and discussion

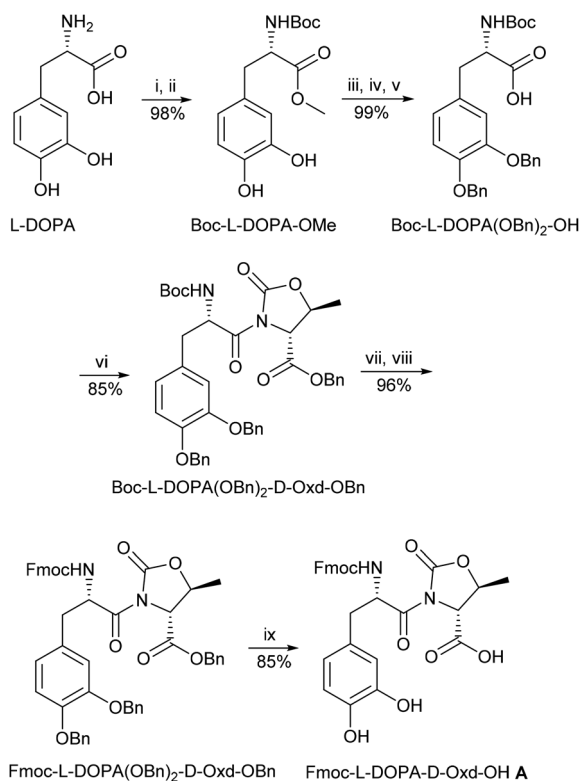
Synthesis of gelator **A**

The synthesis of gelator **A** started from unprotected and commercially available L-DOPA, which was subsequently transformed into Boc-L-DOPA(OBn)₂-OH over five steps on a multi-gram scale with excellent yields, following a literature procedure.^{36,37} Further steps allowed us to introduce the D-Oxd moiety, to replace the Boc moiety with the Fmoc moiety and to remove the three benzyl protecting groups (Scheme 1). The gelator **A** was obtained pure as a white solid in an overall yield of 67% from L-DOPA. Compounds **B** and **C** have been efficiently prepared on a multi-gram scale, following literature procedures.^{30,31}

Hydrogel formation

A systematic study on the ability of compounds **A**, **B** and **C** to form hydrogels was then undertaken to check the importance of the cresol moiety, as a comparison with a phenol or a phenyl group. The presence of two *ortho*-hydroxyl groups should in principle favour its interaction with metal cations due to their chelation ability. The study of the ability to form metal : peptide complexes with zinc will be of particular interest, as zinc is an essential biological co-factor that plays a critical role in the central nervous system.^{38,39} The concentration of intracellular zinc typically ranges between 180 and 250 mM in eukaryotic cells. However, very little zinc exists as 'free' ions within the cell, usually at pico- to low nanomolar concentrations.⁴⁰

We tested the behaviour of zinc cations as triggers to check if they can induce the formation of strong hydrogels with gelators **A**, **B** and **C**. We also compared these results with the be-



Scheme 1 Reagents and conditions: (i) SOCl_2 (excess), MeOH, 0 °C, 24 h; (ii) Boc_2O (2 equiv.), NaHCO_3 (2 equiv.), THF/ H_2O , r.t., 18 h; (iii) BnBr (2.2 equiv.), K_2CO_3 (2.2 equiv.), TBAB (0.2 equiv.), NaI (0.2 equiv.), acetone, reflux, 4 h; (iv) 1 M NaOH, MeOH/THF, r.t., 18 h; (v) 1 M HCl; (vi) *D*-Oxd-OBn (1 equiv.), HBTU (1.1 equiv.), DIEA (2 equiv.), AcCN, r.t., 4 h; (vii) TFA (18 equiv.), CH_2Cl_2 , r.t., 4 h; (viii) Fmoc-NHS (1 equiv.), DIEA (3 equiv.), r.t., 24 h; (ix) Pd/C (10% w/w), H_2 , MeOH/TFA (95 : 5), r.t., 90 min.

haviour of other triggers: divalent and trivalent metal cations (Ca^{2+} , Ba^{2+} , Mg^{2+} , Cu^{2+} , Al^{3+} and Fe^{3+}) and two basic amino acids (histidine and arginine), as we recently demonstrated that they can induce the formation of physical hydrogels with selected gelators *via* coordination with the gelator carboxylate anions.^{41,42} We also analysed the hydrogels obtained using pH as a trigger upon the addition of a stoichiometric amount of δ -gluconolactone (GdL).⁴³

All the hydrogels were prepared at a 2% w/w gelator concentration, which we recognized as the optimal concentration for strong hydrogel formation.^{30,41,44} The general method for hydrogel preparation was to place a portion (20 mg) of gelator **A**, **B** or **C** in a test tube with 1 mL of MilliQ water (for the GdL and metal cations triggers, a stoichiometric amount of 1 M NaOH is also required). The mixture was then stirred until sample dissolution, the trigger was added to the solution under rapid stirring and the tube was allowed to stand quietly until gel formation occurred. While a stoichiometric amount of GdL or of a given amino acid is needed for strong gel formation, a stoichiometric trigger/gelator ratio of the metal cation did not always provide the best results.⁴⁵ We recently demonstrated that a 0.3 trigger/gelator ratio affords strong hydrogels using calcium chloride as a trigger.⁴²

We checked whether hydrogels were formed under thirty different conditions using **A**, **B** or **C** and ten triggers, however, we were able to prepare only eighteen hydrogels. Although we are aware that the modification of the trigger/gelator ratio may afford interesting results, in this preliminary study, we chose to screen the triggers only under given conditions to focus the investigation on the gelation efficiency as a function of the number of hydroxyl groups in the gelator. All the experiments are summarized in Table 1 and the hydrogels formed have been numbered. All the details are reported in Table S1.†

GdL, CaCl_2 and ZnCl_2 allow the formation of hydrogels with all the gelators studied. In contrast BaCl_2 and *L*-Hys result in the formation of hydrogels with gelators **A** and **B** only, while MgCl_2 allows the gelation of only **B** and **C**. Finally, $\text{Al}_2(\text{SO}_4)_3$, $\text{Fe}(\text{NO}_3)_3$ and *L*-Arg furnish unsatisfactory results. Several hydrogels show a thixotropic behaviour on the macroscopic scale as they become liquid if shear stress is applied and quickly recover their solid form on resting.^{46,47}

Hydrogel characterization

We have recently demonstrated that good rheological properties are usually associated with a higher T_{gel} ,³⁰ hence the first screening of the optimal conditions for hydrogel formation may be conducted using this method. We measured the T_{gel} for all the eighteen hydrogels formed using the dropping ball method (see Experimental and Table S1† for the details), obtaining results ranging between 40 °C and 98 °C. Hydrogels 1–9, obtained with GdL, CaCl_2 or ZnCl_2 always have a T_{gel} higher than 60 °C. Among them, the ZnCl_2 containing hydrogels 7–9 afforded the best results, with a T_{gel} higher than 89 °C. In contrast, no considerable T_{gel} variation may be ascribed to the gelator.

Another interesting parameter that needs to be checked in hydrogel formation is the final pH as a neutral pH is very important for the preparation of biocompatible hydrogels. Among the three most interesting triggers, GdL produces hydrogels 1–3 with the pH ranging between 4.0 and 4.5, too low to be biocompatible, although these hydrogels may be very useful for other applications. In contrast, all the other hydrogels have a final pH ranging between 6.5 and 7.5, and hence they are all good candidates for biological applications.

Table 1 A summary of the conditions used for hydrogel formation with gelators **A**, **B** and **C**. Only the hydrogels formed have been numbered for clarity

Gelator → trigger ↓	Fmoc-L-Dopa-D-Oxd-OH A	Fmoc-L-Tyr-D-Oxd-OH B	Fmoc-L-Phe-D-Oxd-OH C
GdL	1	2	3
CaCl_2	4	5	6
ZnCl_2	7	8	9
BaCl_2	10	11	—
<i>L</i> -Hys	13	14	—
MgCl_2	—	17	18
CuCl_2	19	—	21
$\text{Al}_2(\text{SO}_4)_3$	—	—	—
$\text{Fe}(\text{NO}_3)_3$	—	—	—
<i>L</i> -Arg	—	—	30



Fig. 2 Photographs of hydrogels 1–9 (from left to right).

After this preliminary screening, we focused our attention on hydrogels 1–9, which were formed using GdL, CaCl_2 or ZnCl_2 as the gelator trigger. These triggers allow hydrogel formation with any gelator. A photograph of these hydrogels is shown in Fig. 2, while photographs of all the other hydrogels are reported in Fig. S1.†

More information on the nature of hydrogels 1–9 was obtained using SEM analysis of the aerogels prepared by freeze-drying the samples (Fig. 3). All the L-DOPA containing aerogels, 1, 4 and 7, are organized as platelets; the L-Tyr containing aerogels, 2, 5 and 8, are organized as dense fibrous networks and finally, the L-Phe containing aerogels, 3, 6 and 9, are organized as locally oriented long strips that cross on a large scale. In any case, the fast formation of all the hydrogels suggests that the self-assembly occurs under kinetic rather than thermodynamic conditions.^{48,49}

Another piece of information on the supramolecular interactions involved in the formation of hydrogels 1–9 may be obtained using ATR-IR spectroscopy of the aerogels samples. More ordered fibers obtained with gelator C (Fig. 4C) produce very reproducible IR spectra, all containing a band at 3330 cm^{-1} , typical of hydrogen bonded NH bonds, another strong stretching band at 1687 cm^{-1} , typical of hydrogen bonded CO bonds, together with a weaker band around 1067 cm^{-1} , which may be attributed to the amide band II. The dense fibrous networks, typical of aerogels 2, 5 and 8, show a more complex pattern (Fig. 4B), where either band I prevails at about 1690 cm^{-1} or band II at about 1600 cm^{-1} . Finally the L-DOPA containing aerogels 1, 4 and 7 (Fig. 4A) have IR spectra where both the amide band I and amide band II are present, together with the NH stretching band at 3325 cm^{-1} .

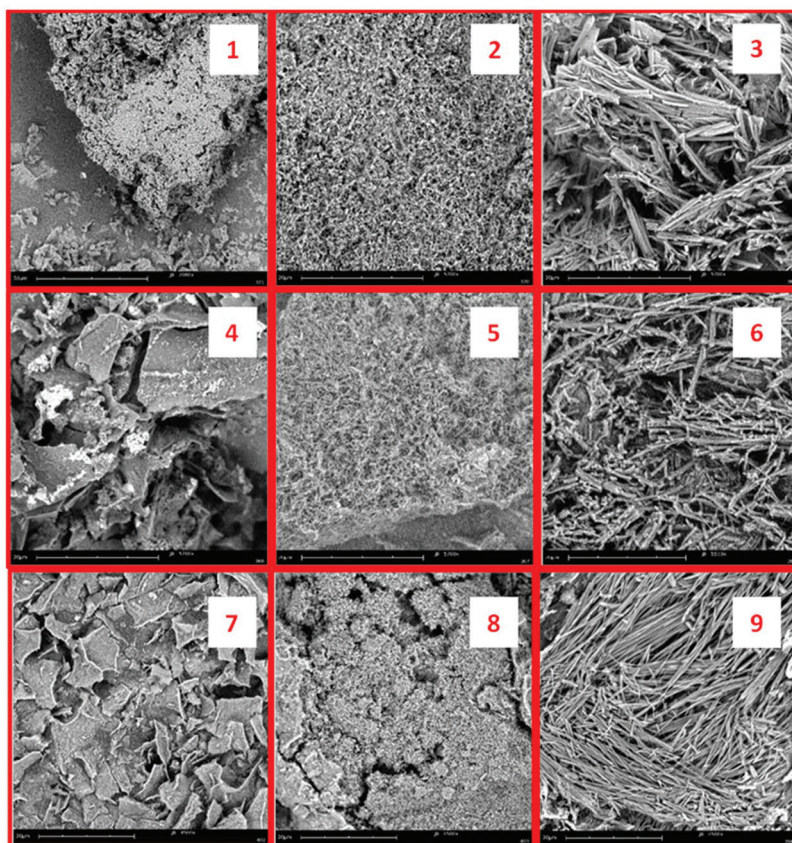


Fig. 3 SEM images of the samples of the xerogels obtained by freeze drying samples of hydrogels 1–9. Scale bar = 20 μm .

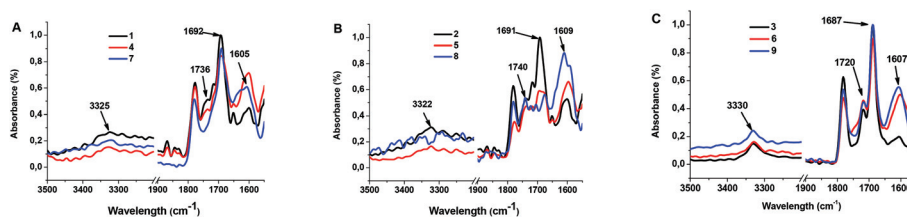


Fig. 4 Selected regions of the ATR-IR spectra of aerogels 1–9: (A) L-DOPA containing aerogels 1, 4 and 7, (B) L-Tyr containing aerogels 2, 5 and 8, and (C) L-Phe containing aerogels 3, 6 and 9.

Rheological analyses were carried out to evaluate the viscoelastic properties of hydrogels 1–9 in terms of the storage and loss moduli (G' and G'' , respectively) (Table 2, Fig. S3–S5†). All the hydrogels obtained were characterized by a storage modulus approximately one order of magnitude higher than

the loss component, indicating their “solid-like” behaviour. Frequency sweep analysis pointed out that for all the hydrogels obtained, both the G' and G'' were almost independent of frequency in the range from 0.1 to 100 rad s^{-1} (with G' always greater than G''), confirming the “solid-like” rheological behaviour.

The rheological studies indicate that the strength of the hydrogels was strongly affected both by the aromatic amino acid and by the trigger. The general trends demonstrate that by maintaining a 0.3 trigger/gelator ratio, the strongest gels were obtained with the L-Tyr containing gelator **B**, as hydrogels 2, 5 and 8 are characterized by storage modulus G' values ranging between 10^4 and 10^5 Pa, with the hydrogel strength following the trend $\text{ZnCl}_2 > \text{GdL} > \text{CaCl}_2$. The L-DOPA containing hydrogels 1, 4 and 7 are characterized by a storage modulus approximately one order of magnitude lower, always ranging between 10^3 and 10^4 Pa, with the hydrogel strength following the trend $\text{CaCl}_2 > \text{GdL} > \text{ZnCl}_2$. This unexpected

Table 2 The rheological properties of hydrogels 1–9

Hydrogel	Gelator	Trigger (equiv.)	G' (Pa)	G'' (Pa)	γ (%)
1	A	GdL (1.1)	3400	430	9.64
2	B	GdL (1.1)	52 600	5000	11.55
3	C	GdL (1.1)	48 800	3440	3.22
4	A	CaCl_2 (0.3)	8500	1050	6.65
5	B	CaCl_2 (0.3)	17 000	2500	5.42
6	C	CaCl_2 (0.3)	6400	430	12.76
7	A	ZnCl_2 (0.3)	2144	366	3.88
8	B	ZnCl_2 (0.3)	74 271	7280	4.69
9	C	ZnCl_2 (0.3)	700	61	6.00

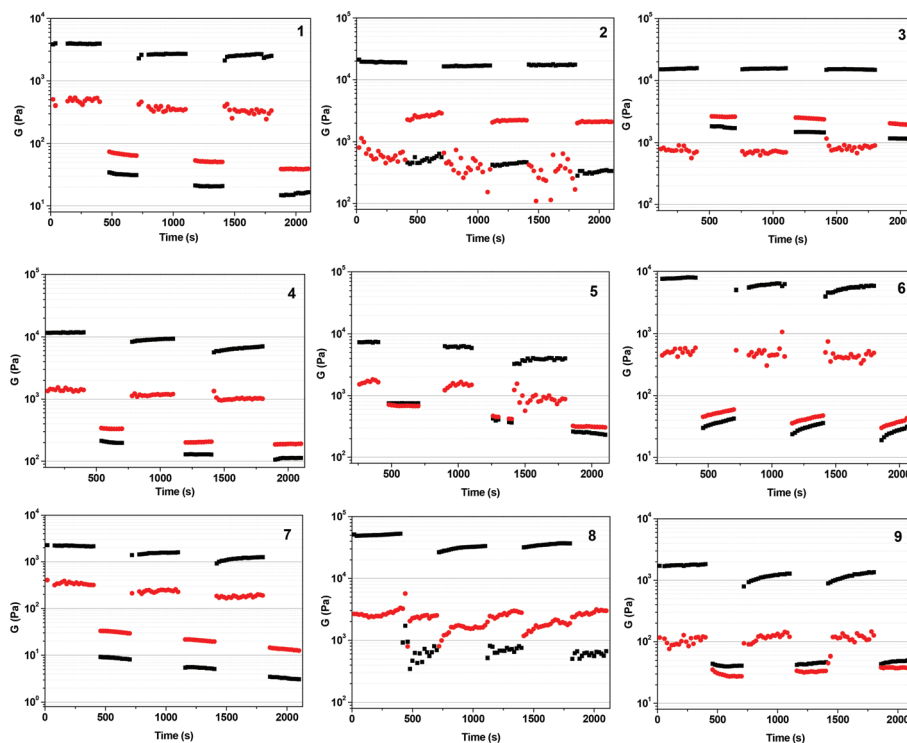


Fig. 5 The values of the storage moduli G' (black) and loss moduli G'' (red) recorded during a step strain experiment performed on hydrogels 1–9.

result may be ascribed to the trigger/gelator ratio, which could be more suitable for gelator **B** rather than for the cresol containing gelator, **A**. We are planning to study the effect of the variation of the trigger/gelator ratio on the hydrogel properties when gelator **A** is used.

Finally, the L-Phe containing gelator **C**, which does not possess any hydroxyl groups, is very sensitive towards the trigger because the hydrogel strength followed the trend $G' > CaCl_2 > ZnCl_2$. These results indicate that there was no universal trigger able to induce the formation of a hydrogel endowed with the best mechanical properties.

Step strain experiments were performed to check the thixotropic behaviour of hydrogels **1–9** on the molecular level. Strain values within and over the crossover point region were consecutively applied to the hydrogels; the hydrogels lost their “solid-like” behavior ($G' < G''$) when the strain applied was over their crossover point region and quickly go back to a “solid-like” state ($G' > G''$) if the strain was in the LVE region the hydrogels (Fig. 5).

Although only hydrogels **3**, **6**, **7**, **8** and **9** show thixotropic behaviour on the macroscopic scale (Table S1†), the results observed for hydrogels **1–9** show that they are all characterized by a great capability to recover the gel-like behaviour, thus showing their thixotropic properties on the molecular level.

Conclusions

We prepared the new gelator Fmoc-L-DOPA-D-Oxd-OH **A** and tested its gelation ability by comparison with the previously reported gelators Fmoc-L-Tyr-D-Oxd-OH **B** and Fmoc-L-Phe-D-Oxd-OH **C** under several gelation conditions, to check the effect of the cresol moiety.

As an overall observation, the different behaviour of the gelators may be attributed to the increased water solubility of the L-DOPA and L-Tyr derivatives compared with the L-Phe containing gelator. The results obtained using the ten different triggers indicate that hydrogel formation was very sensitive to both the number of the hydroxyl moieties linked to the aromatic rings and the nature of the trigger; therefore, there was no common trigger able to produce the hydrogel with the best mechanical properties in any case.

GdL, $CaCl_2$ and $ZnCl_2$ form strong hydrogels endowed with thixotropic behaviour on the molecular level with all the three gelators studied. The analysis of the aerogels obtained by freeze drying the hydrogels show that the three gelators induce the formation of dense networks, as the **A** aerogels show a platelet pattern, the **B** aerogels display an unordered dense fibrous network and the **C** aerogels are organized in locally oriented long strips. Rheological analysis of these samples demonstrated that the strongest hydrogels were obtained with the L-Tyr containing gelator **B**, while the L-DOPA containing hydrogels **1**, **4** and **7** were characterized by a storage modulus approximately one order of magnitude lower. Finally, the strength of the L-Phe containing hydrogels show a different trigger dependency with respect to the other gelators.

Although the fast formation of all the hydrogels suggests that the self-assembly occurs under kinetic rather than thermodynamic conditions, more studies are planned to obtain a deeper understanding of the hydrogelation process responsible for the formation of stronger hydrogels using the L-Tyr gelator **B** compared to the gels formed with the L-DOPA gelator **A**. Moreover, the variation of the trigger/gelator ratio may modify these results, as a different amount of Ca^{2+} or Zn^{2+} may be more suitable for hydrogel formation in the presence of the cresol moiety.

Finally, the strong $ZnCl_2$ containing hydrogels **7–9** suggest that the three gelators have a good propensity to form complexes with this metal. Further studies are currently ongoing to find the optimal gelator/ $ZnCl_2$ ratio for the formation of strong and thixotropic hydrogels for biological and cell growth applications.

Acknowledgements

We gratefully acknowledge the Ministero dell'Università e della Ricerca (PRIN 2015 project 20157WW5EH) and Alma Mater Studiorum Università di Bologna for financial support.

References

- 1 S. Guha, M. G. B. Drew and A. Banerjee, *Chem. Mater.*, 2008, **20**, 2282–2290.
- 2 S. K. Maji, D. Haldar, A. Banerjee and A. Banerjee, *Tetrahedron*, 2002, **58**, 8695–8702.
- 3 S. K. Maji, M. G. Drew and A. Banerjee, *Chem. Commun.*, 2001, 1946–1947.
- 4 R. V. Ulijn and A. M. Smith, *Chem. Soc. Rev.*, 2008, **37**, 664–675.
- 5 F. Rúa, S. Boussert, T. Parella, I. Díez-Pérez, V. Branchadell, E. Giralt and R. M. Ortuño, *Org. Lett.*, 2007, **9**, 3643–3645.
- 6 T. A. Martinek, A. Hetényi, L. Fulop, I. M. Mándity, G. K. Tóth, I. Dékány and F. Fülöp, *Angew. Chem., Int. Ed.*, 2006, **45**, 2396–2400.
- 7 Q. Zou, M. Abbas, L. Zhao, S. Li, G. Shen and X. Yan, *J. Am. Chem. Soc.*, 2017, **139**, 1921–1927.
- 8 M. Abbas, Q. Zou, S. Li and X. Yan, *Adv. Mater.*, 2017, **29**, 1605021.
- 9 K. Liu, R. Xing, Q. Zou, G. Ma, H. Mohwald and X. Yan, *Angew. Chem., Int. Ed.*, 2016, **55**, 3036–3039.
- 10 X. Liu, J. Fei, A. Wang, W. Cui, P. Zhu and J. Li, *Angew. Chem., Int. Ed.*, 2017, **56**, 2660–2663.
- 11 F. E. Cohen and J. W. Kelly, *Nature*, 2003, **426**, 905–909.
- 12 J. Sato, T. Takahashi, H. Oshima, S. Matsumura and H. Mihara, *Chem. – Eur. J.*, 2007, **13**, 7745–7752.
- 13 R. Mishra, B. Bulic, D. Sellin, S. Jha, H. Waldmann and R. Winter, *Angew. Chem., Int. Ed.*, 2008, **47**, 4679–4682.
- 14 A. Fernandez-Barbero, I. J. Suarez, B. Sierra-Martin, A. Fernandez-Nieves, F. J. de las Nieves, M. Marquez, J. Rubio-Retama and E. Lopez-Cabarcos, *Adv. Colloid Interface Sci.*, 2009, **147–148**, 88–108.
- 15 Y. Liu, H. Meng, Z. Qian, N. Fan, W. Choi, F. Zhao and B. P. Lee, *Angew. Chem., Int. Ed.*, 2017, **56**, 4224–4228.

- 16 P. Kord Forooshani and B. P. Lee, *J. Polym. Sci., Part A: Polym. Chem.*, 2017, **55**, 9–33.
- 17 Z. Q. Lei, H. P. Xiang, Y. J. Yuan, M. Z. Rong and M. Q. Zhang, *Chem. Mater.*, 2014, **26**, 2038–2046.
- 18 X. Dai, Y. Zhang, L. Gao, T. Bai, W. Wang, Y. Cui and W. Liu, *Adv. Mater.*, 2015, **27**, 3566–3571.
- 19 Y. Hu, W. Guo, J. S. Kahn, M. A. Aleman-Garcia and I. Willner, *Angew. Chem., Int. Ed.*, 2016, **55**, 4210–4214.
- 20 M. Nakahata, Y. Takashima, H. Yamaguchi and A. Harada, *Nat. Commun.*, 2011, **2**, 1–6.
- 21 G. Angelici, N. Castellucci, G. Falini, D. Huster, M. Monari and C. Tomasini, *Cryst. Growth Des.*, 2010, **10**, 923–929.
- 22 G. Angelici, G. Falini, H. J. Hofmann, D. Huster, M. Monari and C. Tomasini, *Chem. – Eur. J.*, 2009, **15**, 8037–8048.
- 23 G. Angelici, N. Castellucci, S. Contaldi, G. Falini, H. J. Hofmann, M. Monari and C. Tomasini, *Cryst. Growth Des.*, 2010, **10**, 244–251.
- 24 N. Castellucci, G. Sartor, N. Calonghi, C. Parolin, G. Falini and C. Tomasini, *Beilstein J. Org. Chem.*, 2013, **9**, 417–424.
- 25 N. Castellucci, G. Angelici, G. Falini, M. Monari and C. Tomasini, *Eur. J. Org. Chem.*, 2011, 3082–3088.
- 26 N. Castellucci, G. Falini, G. Angelici and C. Tomasini, *Amino Acids*, 2011, **41**, 609–620.
- 27 S. Lucarini and C. Tomasini, *J. Org. Chem.*, 2001, **66**, 727–732.
- 28 C. Tomasini, V. Trigari, S. Lucarini, F. Bernardi, M. Garavelli, C. Peggion, F. Formaggio and C. Toniolo, *Eur. J. Org. Chem.*, 2003, **4**, 259–267.
- 29 G. Angelici, G. Luppi, B. Kaptein, Q. B. Broxterman, H. J. Hofmann and C. Tomasini, *Eur. J. Org. Chem.*, 2007, 2713–2721.
- 30 N. Zanna, A. Merlettini, G. Tatulli, L. Milli, M. L. Focarete and C. Tomasini, *Langmuir*, 2015, **31**, 12240–12250.
- 31 L. Milli, N. Castellucci and C. Tomasini, *Eur. J. Org. Chem.*, 2014, 5954–5961.
- 32 K. L. Morris, L. Chen, A. Rodger, D. J. Adams and L. C. Serpell, *Soft Matter*, 2015, **11**, 1174–1181.
- 33 G. Fichman and E. Gazit, *Acta Biomater.*, 2014, **10**, 1671–1682.
- 34 B. Adhikari, J. Nanda and A. Banerjee, *Chem. – Eur. J.*, 2011, **17**, 11488–11496.
- 35 L. Chen, K. Morris, A. Laybourn, D. Elias, M. R. Hicks, A. Rodger, L. Serpell and D. J. Adams, *Langmuir*, 2010, **26**, 5232–5242.
- 36 A. Gaucher, L. Dutot, O. Barbeau, W. Hamchaoui, M. Wakselman and J. P. Mazaleyrat, *Tetrahedron: Asymmetry*, 2005, **16**, 857–864.
- 37 G. E. Magoulas, A. Rigopoulos, Z. Piperigkou, C. Gialeli, N. K. Karamanos, P. G. Takis, A. N. Troganis, A. Chrissanthopoulos, G. Maroulis and D. Papaioannou, *Bioorg. Chem.*, 2016, **66**, 132–144.
- 38 K. L. Veldkamp, P. J. Tubergen, M. A. Swartz, J. T. DeVries and C. D. Tatko, *Inorg. Chim. Acta*, 2017, **461**, 120–126.
- 39 F. Burnett, *Lancet*, 1981, **317**, 186–188.
- 40 R. D. Palmiter and S. D. Findley, *EMBO J.*, 1995, **14**, 639–649.
- 41 N. Zanna, A. Merlettini and C. Tomasini, *Org. Chem. Front.*, 2016, **3**, 1699–1704.
- 42 N. Zanna, S. Focaroli, A. Merlettini, L. Gentilucci, G. Teti, M. Falconi and C. Tomasini, *ACS Omega*, 2017, **2**, 2374–2381.
- 43 D. J. Adams, M. F. Butler, W. J. Frith, M. Kirkland, L. Mullen and P. Sanderson, *Soft Matter*, 2009, **5**, 1856–1862.
- 44 L. Milli, N. Zanna, A. Merlettini, M. Di Giosia, M. Calvaresi, M. L. Focarete and C. Tomasini, *Chem. – Eur. J.*, 2016, 12106–12112.
- 45 L. Chen, G. Pont, K. Morris, G. Lotze, A. Squires, L. C. Serpell and D. J. Adams, *Chem. Commun.*, 2011, **47**, 12071–12073.
- 46 Y. Li, F. Zhou, Y. Wen, K. Liu, L. Chen, Y. Mao, S. Yang and T. Yi, *Soft Matter*, 2014, **10**, 3077–3085.
- 47 J. Mewis and N. J. Wagner, *Adv. Colloid Interface Sci.*, 2009, **147–148**, 214–227.
- 48 J. Wang, K. Liu, L. Yan, A. Wang, S. Bai and X. Yan, *ACS Nano*, 2016, **10**, 2138–2143.
- 49 J. Wang, K. Liu, R. Xing and X. Yan, *Chem. Soc. Rev.*, 2016, **45**, 5589–5604.